Supporting Information

Boosting oxygen evolution reaction activity of perovskite through introducing multi-elements synergy and building ordered structure

Hainan Sun[a], Xiaomin Xu[b], Zhiwei Hu[c], Liu Hao Tjeng[c], Jie Zhao[a], Qin Zhang[d], Hong-Ji Lin[e], Chien-Te Chen[e], Ting-Shan Chan[e], Wei Zhou[a,*], and Zongping Shao[a,b,*]

[a] State Key Laboratory of Materials-Oriented Chemical Engineering, College of Chemical Engineering, Nanjing Tech University, Nanjing 211816, P. R. China

[b] Department of Chemical Engineering, Curtin University, Perth, Western Australia 6845, Australia

[c] Max-Planck-Institute for Chemical Physical of Solids, Nöthnitzer Street 40, Dresden 01187, Germany

[d] School of Science, Shandong Jiaotong University, Jinan 250357, P. R. China

[e] National Synchrotron Radiation Research Center, 101 Hsin-Ann Road, Hsinchu 30076, Taiwan

*Corresponding author: E-mail addresses

zhouwei1982@njtech.edu.cn (Wei Zhou)

shaozp@njtech.edu.cn (Zongping Shao)

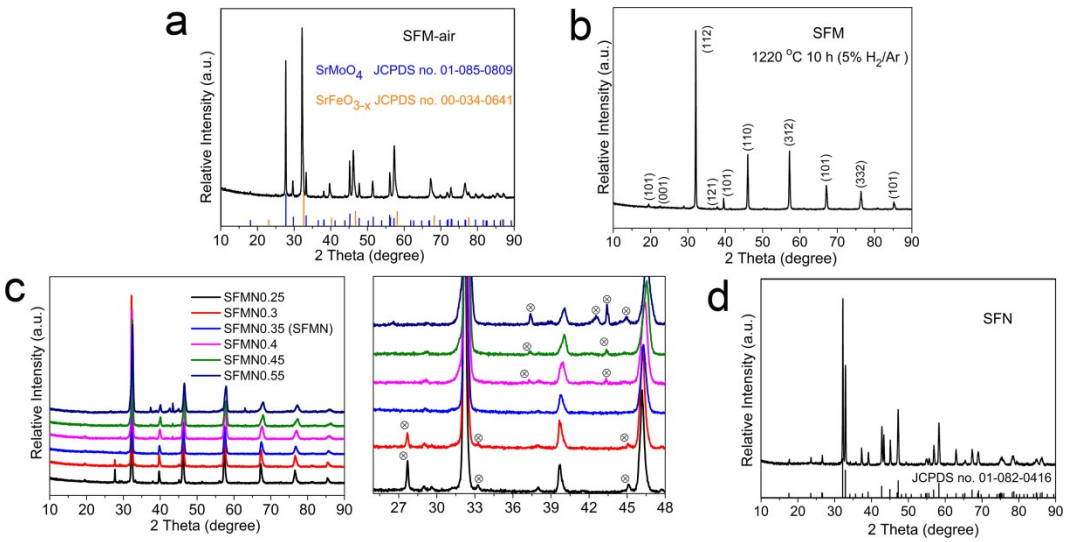

Figure S1. Room-temperature XRD patterns of (a) SFM-air, (b) SFM, (c) SFMNx (x = 0.25, 0.3, 0.35, 0.4, 0.45 and 0.55) along with the magnified XRD spectrum of SFMNx between 2-theta of 26 and 48 °. The marks represent the $SrMoO_4$ phase formation. (d) SFN along with the corresponding reference spectra of $Sr_3Fe_{1.5}Ni_{0.5}O_{7-\delta}$.

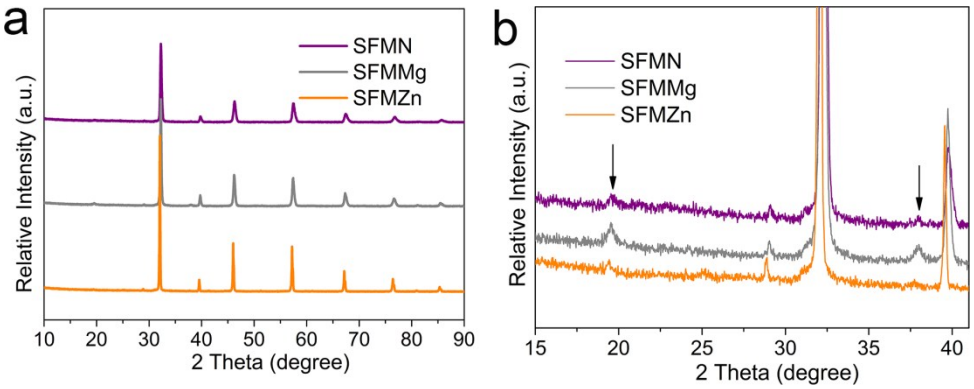

Figure S2. Room-temperature XRD patterns of (a) SFMN, SFMMg, and SFMZn. (b) Magnified XRD spectrum of SFMN, SFMMg, and SFMZn between 2-theta of 15 and 42 °. The arrows represent the characteristic peaks of the B-site cations ordered double perovskite structure.

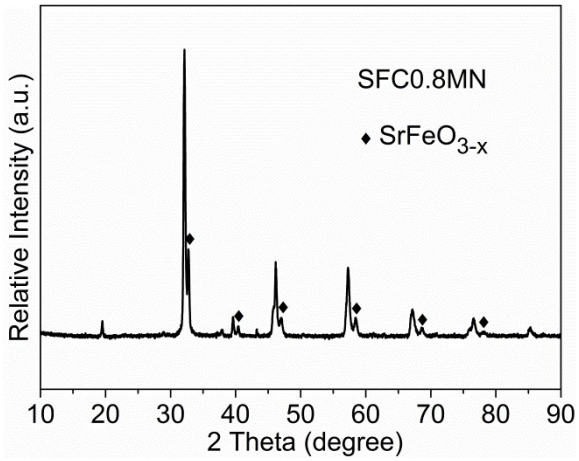

Figure S3. Room-temperature XRD patterns of SFC0.8MN.

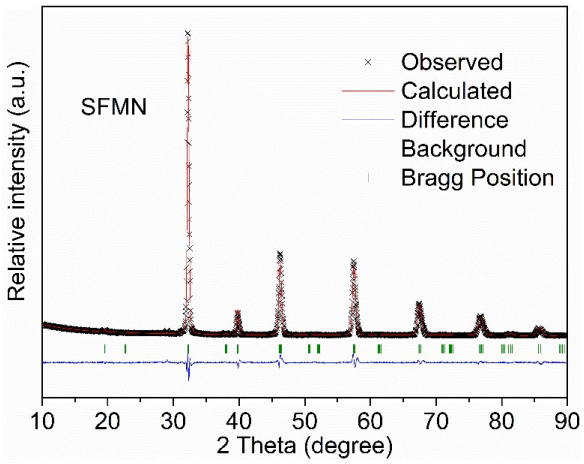

Figure S4. Rietveld refinement XRD patterns of SFMN.

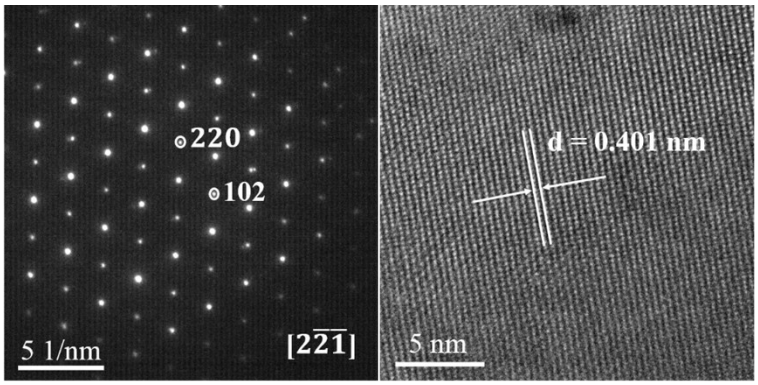

Figure S5. SAED pattern and the corresponding HR-TEM image for SFCMN.

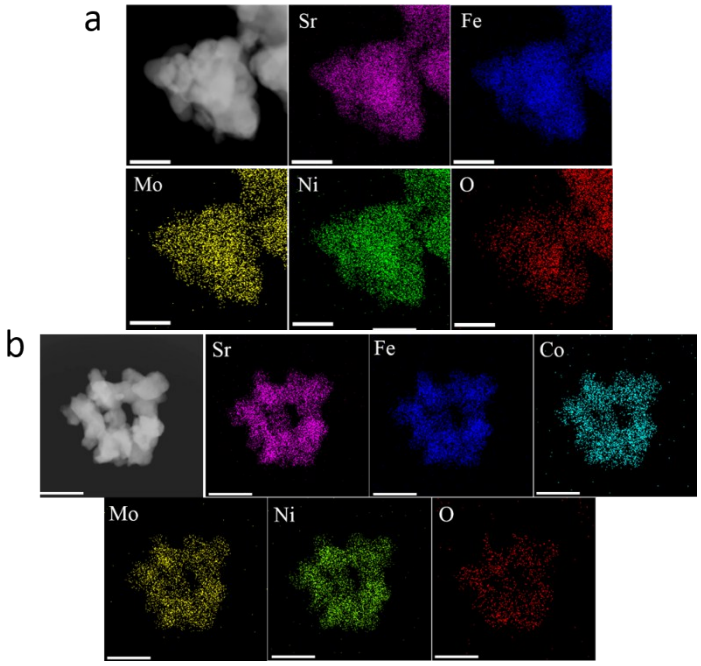

Figure S6. HAADF-STEM image and elemental mapping of Sr, Fe, (Co), Mo, Ni, and O. (a) SFMN, (b) SFCMN. The Scale bar is 250 nm.

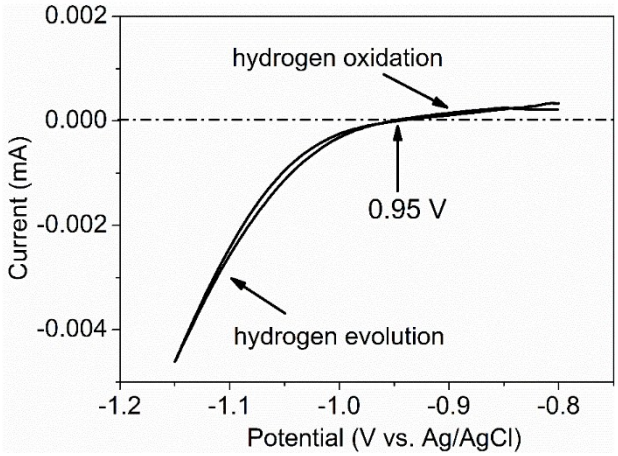

Figure S7. Potential calibration of the reference electrode (Ag/AgCl) in 0.1 M KOH solution. In summary, the potentials in the main text were calibrated by the following equation: $V_{RHE} = V_{Ag/AgCl} + 0.95$ V.

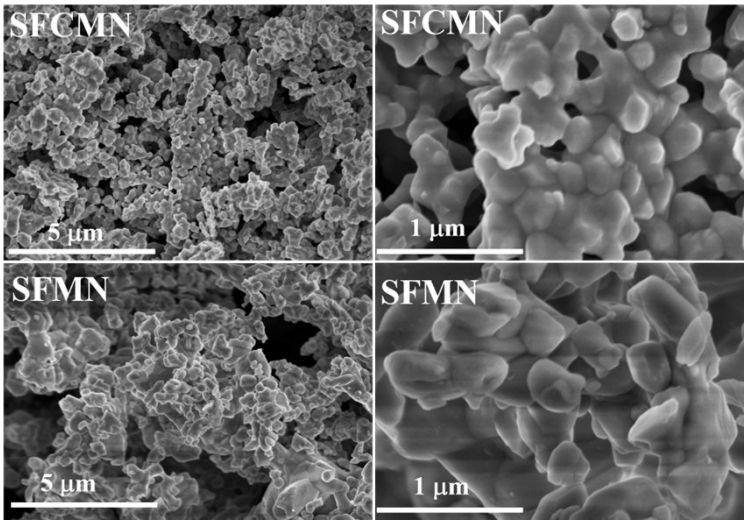

Figure S8. SEM images of the SFCMN and SFMN with different magnifications.

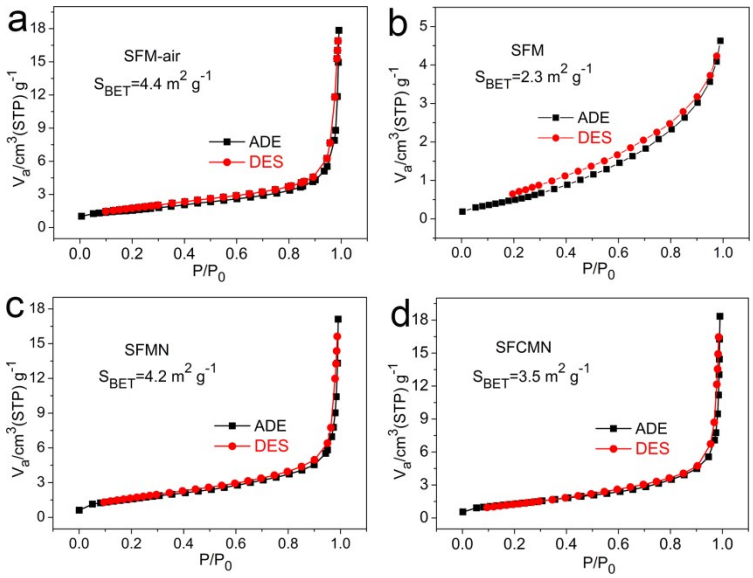

Figure S9. Nitrogen adsorption-desorption isotherm curves and their corresponding surface area of (a) SFM-air, (b) SFM, (c) SFMN and (d) SFCMN.

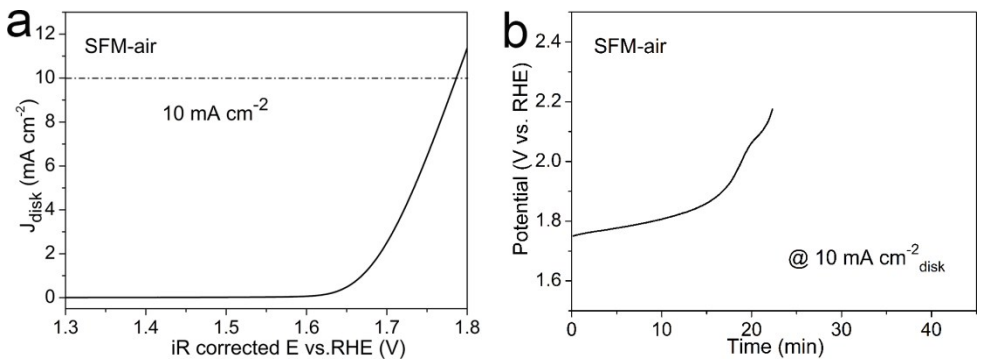

Figure S10. (a) OER activities collected from LSVs of SFM-air catalyst in O_2-saturated 0.1 M KOH solution. (b) CP responses of the SFM-air catalyst on the RDE at a constant current density of 10 mA cm^{-2}_{disk} in O_2-saturated 0.1 M KOH solution.

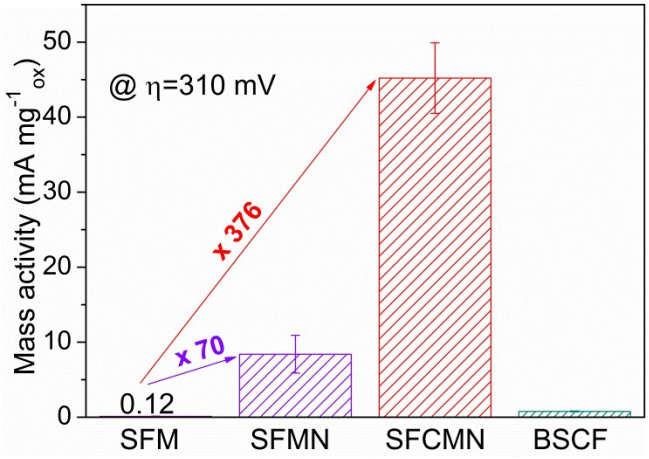

Figure S11. OER mass activity of the SFM, SFMN, SFCMN, and BSCF catalysts at overpotential of 310 mV. Error bars are the standard deviations of measurements done in triplicate.

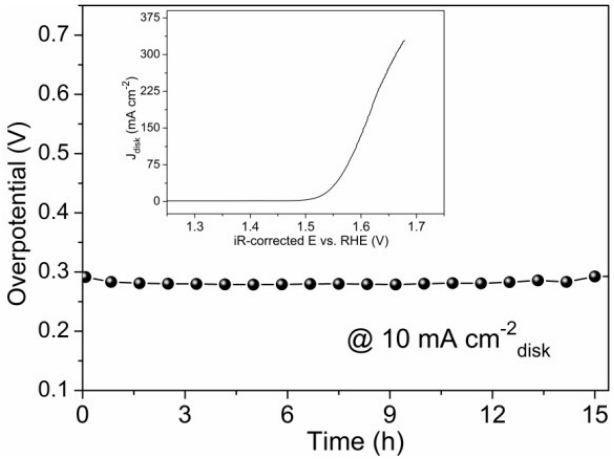

Figure S12. CP responses of SFCMN catalyst on the RDE at a constant current density of 10 mA cm^{-2}_{disk} in 1.0 M KOH. The OER activity collected from LSVs of SFCMN catalyst in O_2-saturated 1.0 M KOH solution is shown as an inset.

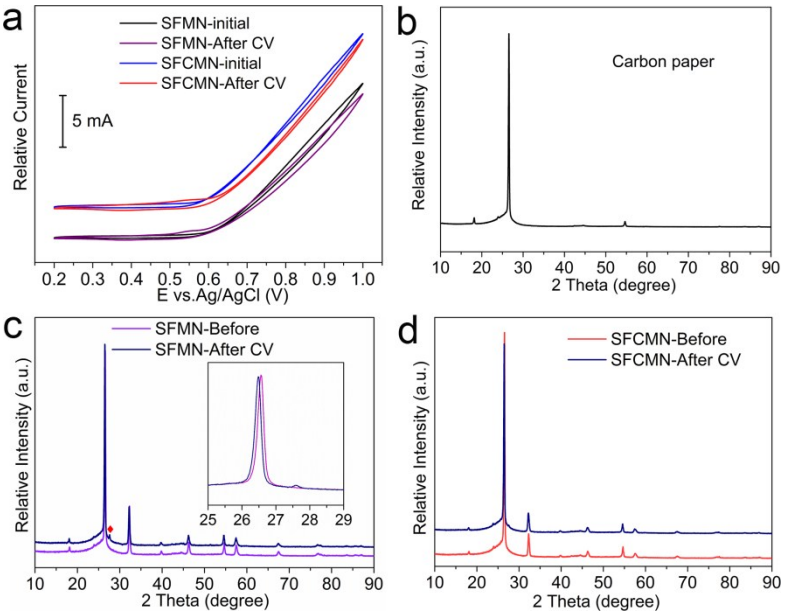

Figure S13. (a) Cyclic voltammetry (CV) curves of SFMN and SFCMN before and after the CV test. (b) XRD pattern of carbon paper (serving as substrate) for comparison. (c) XRD pattern of SFMN before and after the CV test supported on carbon paper. Inset is a magnified XRD pattern. (d) XRD pattern of SFCMN before and after the CV test supported on carbon paper.

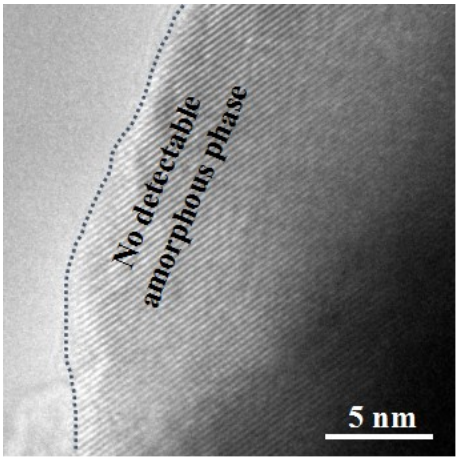

Figure S14. High resolution TEM image of SFCMN after CV test.

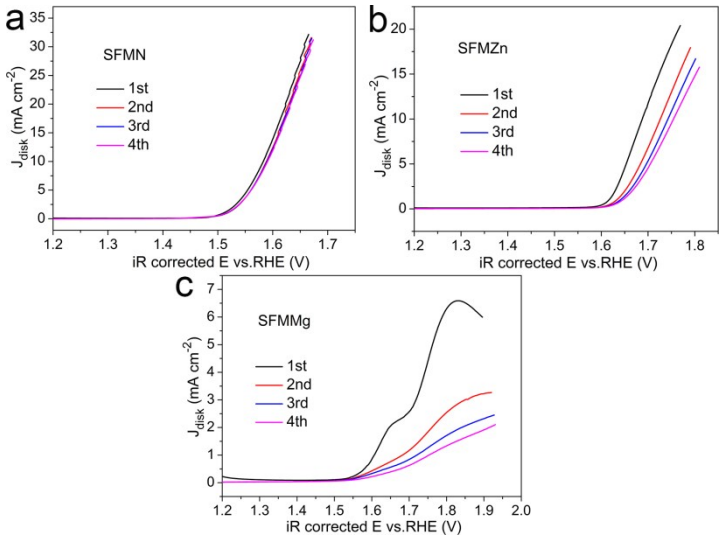

Figure S15. The first four LSV profiles for SFMN (a), SFMZn (b) and SFMMg (c), respectively. LSVs for the OER activities were tested in O_2-saturated 0.1 M KOH solution at a scan rate of 1600 rpm.

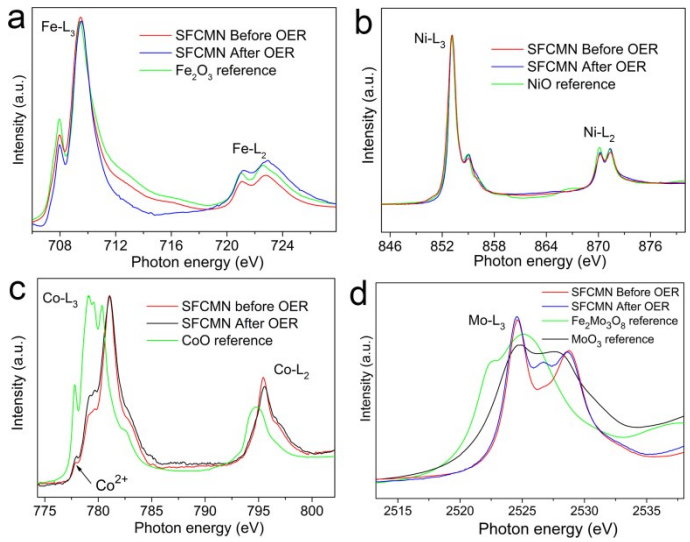

Figure S16. The XAS spectra of SFCMN before and after OER at (a) the Fe $L_{2,3}$ edges; (b) the Ni $L_{2,3}$ edges; (c) the Co $L_{2,3}$ edges; (d) the Mo L_3 edge. The XAS spectra of corresponding references are also shown for comparison.

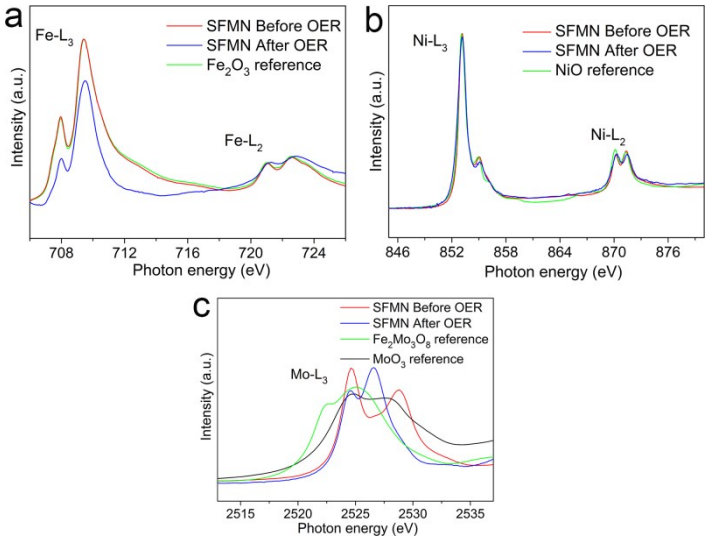

Figure S17. The XAS spectra of SFMN before and after OER at (a) the Fe $L_{2,3}$ edges; (b) the Ni $L_{2,3}$ edges; (c) the Mo L_3 edge. The XAS spectra of corresponding references are also shown for comparison.

The Fe^{3+}, Ni^{2+}, and Mo^{5+}/Mo^{6+} states in SFMN have been confirmed by soft XAS, and Sr in the A-site is divalent. In addition, the valence state of Mo ion is very close to 6+. Then, according to the charge balance ($2 \times 2(Sr^{2+})+1 \times 3(Fe^{3+})+0.65 \times 6(Mo^{6+})+0.35 \times 2(Ni^{2+})=2 \times (6-\delta)(O^{2-})$), we obtain

$\delta \approx 0.20$ in $Sr_2FeMo_{0.65}Ni_{0.35}O_{6-\delta}$. Besides, Co ion is $Sr_2Fe_{0.8}Co_{0.2}Mo_{0.65}Ni_{0.35}O_{6-\delta}$ is mixed valence of Co^{2+} and Co^{3+} and Co doping has a negligible effect on the state of Fe, Ni and Mo compared to $Sr_2FeMo_{0.65}Ni_{0.35}O_{6-\delta}$. Therefore, the partial substitution of Fe (Fe^{3+}) by Co (Co^{2+} and Co^{3+}) in SFCMN can enhance the formation of oxygen vacancies. According to the charge balance ($2 \times 2(Sr^{2+}) +0.8 \times 3(Fe^{3+})+0.2 \times 2.8(Co^{2+}/Co^{3+})+0.65 \times 6(Mo^{6+})+0.35 \times 2(Ni^{2+})=2 \times (6-\delta)(O^{2-})$), we obtain $\delta \approx 0.22$ in $Sr_2Fe_{0.8}Co_{0.2}Mo_{0.65}Ni_{0.35}O_{6-\delta}$.

Table S1. As-synthesized catalysts with their nominal compositions, calcination condition, and abbreviations, respectively.

Catalysts	Calcination Condition	Atmosphere	Abbreviation
$Sr_2FeMoO_{6-\delta}$	1100 °C/10 h	Air	SFM-air
$Sr_2FeMoO_{6-\delta}$	1220 °C/10 h	5% H_2/Ar	SFM
$Sr_2FeNiO_{6-\delta}$	1000 °C/10 h	Air	SFN
$Sr_2FeMo_{0.75}Ni_{0.25}O_{6-\delta}$	1100 °C/10 h	Air	SFMN0.25
$Sr_2FeMo_{0.7}Ni_{0.3}O_{6-\delta}$	1100 °C/10 h	Air	SFMN0.3
$Sr_2FeMo_{0.65}Ni_{0.35}O_{6-\delta}$	1100 °C/10 h	Air	SFMN
$Sr_2FeMo_{0.6}Ni_{0.4}O_{6-\delta}$	1100 °C/10 h	Air	SFMN0.4
$Sr_2FeMo_{0.55}Ni_{0.45}O_{6-\delta}$	1100 °C/10 h	Air	SFMN0.45
$Sr_2FeMo_{0.45}Ni_{0.55}O_{6-\delta}$	1100 °C/10 h	Air	SFMN0.55
$Sr_2FeMo_{2/3}Mg_{1/3}O_{6-\delta}$	1200 °C/10 h	Air	SFMMg
$Sr_2FeMo_{0.63}Zn_{0.37}O_{6-\delta}$	1150 °C/10 h	Air	SFMZn
$Sr_2Fe_{0.8}Co_{0.2}Mo_{0.65}Ni_{0.35}O_{6-\delta}$	1100 °C/10 h	Air	SFCMN
$Sr_2Fe_{0.2}Co_{0.8}Mo_{0.65}Ni_{0.35}O_{6-\delta}$	1100 °C/10 h	Air	SFC0.8MN
$Ba_{0.5}Sr_{0.5}Co_{0.8}Fe_{0.2}O_{3-\delta}$	1000 °C/5 h	Air	BSCF

Table S2. Summary of structure parameters for the as-synthesized SFMN from Rietveld refinement (space group I 4/m) at room temperature.

a = b/c (Å)	5.56126(5)/7.82912(6)
V (Å^3)	242.135(9)
χ^2/R_{wp}(%)/R_p(%)	4.715/4.33/3.11

Table S3. Crystallographic details of SFMN obtained from neutron powder diffraction data.

Space group: *I/4m*						
Lattice parameter a = b = 5.5720(7)Å, c = 7.8386(8)Å, vol = 243.37(5) Å^3						
Atom	Site	x	y	z	U_{iso} (Å^2)	Occupancy
Sr	4	0	0.5	0.25	0.0108(4)	1
Fe	2	0	0	0	0.0001(1)	1
Mo	2	0	0	0.5	0.0100(0)	0.668
Ni	2	0	0	0.5	0.0100(0)	0.332
O1	4	0	0	0.254	0.0158(5)	1
O2	8	0.233	0.27	0	0.0102(5)	1
wR = 4.99 %						

Table S4. Metal elements compositions by ICP-MS of the SFMN and SFCMN powders

ICP-MS analysis						
Nominal composition	The concentrations of metal ions (mg L^{-1})					ICP-MS composition
	Sr	Fe	Co	Mo	Ni	
$Sr_2FeMo_{0.65}Ni_{0.35}O_{6-\delta}$	4.071	1.164	/	1.333	0.409	$Sr_{2.08}FeMo_{0.67}Ni_{0.34}O_{6-\delta}$
$Sr_2Fe_{0.8}Co_{0.2}Mo_{0.65}Ni_{0.35}O_{6-\delta}$	3.373	0.705	0.185	0.959	0.314	$Sr_{2.07}Fe_{0.8}Co_{0.2}Mo_{0.64}Ni_{0.34}O_{6-\delta}$

Table S5. Comparison of OER catalytic activity data with various recently reported catalysts.

Catalysts	Onset overpotential (mV)	Overpotential (mV) @ 10 mA cm^{-2}	Tafel slope (mV dec^{-1})	Ref.
IrO_2	240	450	83	This work
RuO_2	240	390	78	ACS Catal. 2018, 8, 364
$Sr_2FeMoO_{6-\delta}$	368	450	53	This work
$Sr_2FeMo_{0.65}Ni_{0.35}O_{6-\delta}$	252	340	61	This work
$Sr_2Fe_{0.8}Co_{0.2}Mo_{0.65}Ni_{0.35}O_{6-\delta}$	190	310	56	This work
$PrBaCo_2O_{5+\delta}$	315	517	145	Chem. Eur. J. 2017, 23, 5722
$PrBa_{0.85}Ca_{0.15}MnFeO_{5+\delta}$	290	400	88	Chem. Mater., 2017, 29, 6228
$PrBa_{0.5}Sr_{0.5}Co_{1.5}Fe_{0.5}O_{5+\delta}$-ш	260	358	52	Nat. Commun. 2017, 8, 14586
$Ba_{0.5}Sr_{0.5}Co_{0.8}Fe_{0.2}O_{3-\delta}$	310	510	100	Electrochimica. Acta, 2016, 219 553
$BaCo_{0.7}Fe_{0.2}Sn_{0.1}O_{3-\delta}$	300	450	69	Adv. Sci. 2015, 1500187

$Ba_2Bi_{0.1}Sc_{0.2}Co_{1.7}O_{6-\delta}$	310	492	102	Chem. Eur. J. 2017, 23, 5722
$La_{0.3}(Ba_{0.5}Sr_{0.5})_{0.7}Co_{0.8}Fe_{0.2}O_{3-\delta}$	N/A[a]	480	N/A	Angew. Chem. Int. Ed. 2014, 53, 4582
$LaFeO_{3-\delta}$	320	510	77	Chem. Mater. 2016, 28, 1691
$La_{0.95}FeO_{3-\delta}$	320	400	48	Chem. Mater. 2016, 28, 1691
Bulk $LaCoO_3$	370	620	102	Nat. Commun. 2016, 7, 11510
80nm $LaCoO_3$	330	490	69	Nat. Commun. 2016, 7, 11510
$SrCo_{0.95}P_{0.05}O_{3-\delta}$	360	480	84	Adv. Funct. Mater. 2016, 26, 5862
$SrCo_{0.9}Ti_{0.1}O_{3-\delta}$	320	510	88	ACS Appl. Mater. Interfaces 2015, 7, 17663
$SrNb_{0.1}Co_{0.7}Fe_{0.2}O_{3-\delta}$-BM	300	500	76	Angew. Chem. Int. Ed. 2015, 54, 3897
$SrNb_{0.1}Co_{0.7}Fe_{0.2}O_{3-\delta}$-Nanorod	290	389	61	Adv. Energy Mater. 2017, 1602122

Spinels-relative and hydroxides/oxyhydroxides catalysts					
Catalysts	Onset overpotential (mV)	Overpotential (mV) at 10 mA cm^{-2}	Tafel slope (mV dec^{-1})	Electrolyte (M KOH)	Ref.
$Sr_2Fe_{0.8}Co_{0.2}Mo_{0.65}Ni_{0.35}O_{6-\delta}$	190	310	56	0.1	This work
Co_3O_4	270	490	61	0.1	RSC Adv. 2015, 5, 27823
Porous Co_3O_4 nanoplates	284	523	71	1	J. Mater. Chem. A 2015, 3, 8107
Co_3O_4/C nanowires	240	290	70	0.1	J. Am. Chem. Soc. 2014, 136, 13925
Au-meso-Co_3O_4	300	440	46	0.1	ChemSusChem 2014, 7, 82
$Zn_xCo_{3-x}O_4$ nanowires	N/A	320	51	0.1	Chem. Mater. 2014, 26, 1889
$Mn_xCo_{3-x}O_{4-\delta}$	290	350	85	0.1	Chem. Eur. J. 2014, 20, 12669
NiCo LDH nanosheets	290	420	113	0.1	J. Power Sources 2015, 278, 445
NiCo LDH	230	N/A	101	0.1	Nano Lett. 2015, 15, 1421
NiCoFe LDH nanoarray	230	N/A	57	1	Nanoscale 2014, 6, 11789
NiCo LDH/N-doped graphene	250	N/A	614	0.1	Angew. Chem., Int. Ed. 2013, 52, 13567
NiFe LDH	230	N/A	50	0.1	Chem. Commun. 2014, 50, 6479
α-$Ni(OH)_2$	310	331	42	0.1	J. Am. Chem. Soc. 2014, 136, 7077

[a]: N/A = Not available.